EFFECT OF HALL CURRENTS ON CONVECTIVE HEAT TRANSFER IN A VERTICAL WAVY CHANNEL IN THE PRESENCE OF TEMPERATURE DEPENDENT HEAT SOURCE

M. SESHASAILAJA[1] and G.SAROJAMMA[2]

[1] Scholar, [2] Professor

Department of Applied Mathematics,Sri Padmavati Mahila Visvavidyalayam
Tirupati – 517502, Andhrapradesh, India.

ABSTRACT

The convective heat transfer flow of a viscous electrically conducting fluid in a vertical wavy channel under the influence of an inclined magnetic fluid with heat generating sources is investigated. The walls of the channels are maintained at constant temperatures. The non-linear coupled equations governing the flow and heat are solved by employing perturbation technique with a slope δ of the wavy wall. The velocity and temperature distributions are investigated for different values of G, R, β, M, m, N, α and z. The rate of heat transfer is numerically evaluated for different variations of the governing parameters.

Keywords: Heat transfer, Hall currents, Heat generating Sources, Vertical wavy channel, Porous medium.

---

1. INTRODUCTION

In recent years, energy and material saving considerations have prompted an expansion of the efforts at producing efficient heat exchanger equipment through augmentation of heat transfer. It has been established [8] that channels with diverging – converging geometries augment the transportation of heat transfer and momentum. As the fluid flows through a tortuous path viz., the dilated – constricted geometry, there will be more intimate contact between them. The flow takes place both axially (primary) and transversely (secondary) with the secondary velocity being towards the axis in the fluid bulk rather than confining within a thin layer as in straight channels. Hence it is advantageous to go for converging-diverging geometries for improving the design of heat transfer equipment. Vajravelu and Nayfeh [14] have investigated the influence of the wall waviness on friction

and pressure drop of the generated Couette flow. Vajravelu and Sastry [12] have analyzed the free convection heat transfer in a viscous, incompressible fluid confined between long vertical wavy walls in the presence of constant heat source. Later Vajravelu and Debnath [13] have extended this study to convective flow in a vertical wavy channel in four different geometrical configurations. This problem has been extended to the case of wavy walls by Mc Michel and Deutsch [8], Deshikachar et. al., [4] Rao *et. al.,* [10] and Sree Ramachandra Murthy [11]. Hyan Gook Won *et. al.,* [5] have analyzed that the flow and heat/mass transfer in a wavy duct with various corrugation angles in two dimensional flow regimes. Mahdy [7] have studied the mixed convection heat and mass transfer on a vertical wavy plate embedded in a saturated porous medium. Comini *et. al.,* [2] have analyzed the convective heat and mass transfer in wavy finned-tube exchangers. Jer-Huan Jang *et. al.,* [6] have analyzed that the mixed convection heat transfer along a vertical wavy surface.

Heat generation in a porous medium due to the presence of temperature dependent heat sources has number of applications related to the development of energy resources. It is also important in engineering processes pertaining to flows in which a fluid supports an exothermic chemical or nuclear reaction. Disposition of the radioactive waste material burying in the ground or in deep ocean sediment is another problem where heat generation in porous medium occurs. David Molean [3] has studied the effect of temperature dependent heat source which can be noticed in the electrical heating on the steady state transfer within a porous medium. Chandrasekhar [1], Palm [9] presented an extensive review of the forced convection with heat generating source. Mixed convection flows have been studied extensively in various geometrics with different thermal boundary conditions. Due to the superposition of the buoyancy effects on the main flow there is a secondary flow in the form of a vortex re-circulation pattern.

The application of electromagnetic fields in controlling the heat transfer as in aerodynamic heating leads to the study of magneto hydrodynamic heat transfer. The MHD heat transfer has gained significance owing to to its applications in space technology. The MHD heat transfer can be classified into sections. One contains problems in which the heating is an incidental byproduct of the electromagnetic fields as in the MHD generators and pumps etc. and the second contains of problems in which the primary use of electromagnetic fields is to control the heat transfer. With the deepening of fuel crisis all over the world there is a great concern to utilize the enormous power beneath the earth's crust in the geothermal region. Liquid in the geothermal region is an electrically conducting liquid with high temperature. Hence the study of interaction of the geomagnetic field with the fluid in the

geothermal region is of great interest, thus leading to the study of Magnetohydrodynamic convection flows through porous medium.

2. FORMULATION OF THE PROBLEM

We consider the steady flow of an incompressible, viscous, electrically conducting fluid confined in a vertical channel bounded by two wavy walls under the influence of an inclined magnetic field of intensity Ho lying in the plane (y-z). The magnetic field is inclined at an angle α to the axial direction and hence its components are $(0, H_0 Sin(\alpha), H_0 Cos(\alpha))$. In view of the waviness of the wall the velocity field has components (u, 0, w). The magnetic field in the presence of fluid flow induces the current $(J_x, 0, J_z)$.We choose a rectangular Cartesian co-ordinate system O(x, y, z) with z-axis in the vertical direction and the walls at $x = \pm f(\frac{\delta z}{L})$.

The governing equations of motion are

$$u\frac{\partial u}{\partial x} + w\frac{\partial u}{\partial z} = -\frac{\partial p}{\partial x} + \mu(\frac{\partial^2 u}{\partial x^2} + \frac{\partial^2 u}{\partial z^2}) + \\ -\frac{\sigma\mu_e H_{0\,0}^2 Sin^2(\alpha)}{1 + m^2 H_0^2 Sin^2(\alpha)}(u + mH_0 wSin(\alpha)) \tag{2.1}$$

$$u\frac{\partial W}{\partial x} + w\frac{\partial W}{\partial z} = -\frac{\partial p}{\partial z} + \mu(\frac{\partial^2 W}{\partial x^2} + \frac{\partial^2 W}{\partial z^2}) - \\ -\frac{\sigma\mu_e H_0^2 Sin^2(\alpha)}{1 + m^2 H_0^2 Sin^2(\alpha)}(w - mH_0 uSin(\alpha)) - \rho g \tag{2.2}$$

The energy equation is

$$\rho C_p(u\frac{\partial T}{\partial x} + w\frac{\partial T}{\partial z} = k_f(\frac{\partial^2 T}{\partial x^2} + \frac{\partial^2 T}{\partial z^2}) + Q(T_2 - T) - \frac{\partial(q_R)}{\partial x} \tag{2.3}$$

The equation of state is

$$\rho - \rho_0 = -\beta(T - T_o) \tag{2.4}$$

with the usual notation.

The flow is maintained by a constant volume flux for which a characteristic velocity is defined as

$$q = \frac{1}{L}\int_{-Lf}^{Lf} w dx \tag{2.5}$$

The boundary conditions are

$$\text{u= 0, w=0, T= T1 on } x = -f(\frac{\delta z}{L}) \tag{2.6}$$

$$\text{u=0, w=0, T= T}_2 \text{ on } x = f(\frac{\delta z}{L}) \tag{2.7}$$

Eliminating the pressure from equations (2.1) and (2.2) and introducing the stream function ψ as

$$u = -\frac{\partial \psi}{\partial z} \quad , \; w = \frac{\partial \psi}{\partial x} \tag{2.8}$$

The equations (2.1) and (2.2) and (2.3) in terms of ψ is

$$\frac{\partial \psi}{\partial z}\frac{\partial(\nabla^2\psi)}{\partial x} - \frac{\partial \psi}{\partial x}\frac{\partial(\nabla^2\psi)}{\partial z} = \mu\nabla^4\psi + \beta g\frac{\partial(T-T_e)}{\partial x} - (\frac{\sigma\mu_e^2 H_0^2 Sin^2(\alpha)}{1+m^2H_0^2\,Sin^2(\alpha)})\nabla^2\psi \tag{2.9}$$

$$\rho C_p(\frac{\partial \psi}{\partial x}\frac{\partial T}{\partial z} - \frac{\partial \psi}{\partial z}\frac{\partial T}{\partial x} = k_f(\frac{\partial^2 T}{\partial x^2} + \frac{\partial^2 T}{\partial z^2}) + Q(T_2 - T) + \frac{16\sigma^{\bullet}T_e^3}{3\beta_R}\frac{\partial^2 T}{\partial x^2} \tag{2.10}$$

On introducing the following non-dimensional variables

$$(x', z') = (x, z)/L\,, \psi' = \frac{\psi}{qL}, \; \theta = \frac{T - T_2}{T_1 - T_2}$$

The equation of momentum and energy in the non-dimensional form are

$$\nabla^4\psi - M_1^2\nabla^2\psi + \frac{G}{R}(\frac{\partial\theta}{\partial x}) = R(\frac{\partial\psi}{\partial z}\frac{\partial(\nabla^2\psi)}{\partial x} - \frac{\partial\psi}{\partial x}\frac{\partial(\nabla^2\psi)}{\partial z}) \qquad (2.11)$$

$$PR(\frac{\partial\psi}{\partial x}\frac{\partial\theta}{\partial z} - \frac{\partial\psi}{\partial z}\frac{\partial\theta}{\partial x}) = ((1+\frac{4}{3N})\frac{\partial^2 T}{\partial x^2} + \frac{\partial^2 T}{\partial z^2}) - \alpha\theta \qquad (2.12)$$

where

$G = \frac{\beta g\,\Delta T_e L^3}{\nu^2}$ (Grashoff Number), $M^2 = \frac{\sigma\mu_e^2 H_o^2 L^2}{\nu^2}$ (Hartmann Number)
$M_1^2 = \frac{M^2 Sin^2(\alpha)}{1+m^2}$ (Reynolds Number), $P = \frac{\mu C_p}{K_f}$ (Prandtl Number),
$\alpha = \frac{QL^2}{C_p K_f}$, (Heat Source Parameter), $N = \frac{\beta_R k_f}{4\sigma^{\bullet} T_e^3}$ (Radiation parameter)
$P_1 = \frac{3NP}{3N+4}$ $\alpha_1 = \frac{3N\alpha}{3N+4}$

The corresponding boundary conditions are

$$\psi(f) - \psi(-f) = 1$$

$$\frac{\partial\psi}{\partial z} = 0, \frac{\partial\psi}{\partial x} = 0, \theta = 1 \quad \text{at } x = -f(\delta z)$$

$$\frac{\partial\psi}{\partial z} = 0, \frac{\partial\psi}{\partial x} = 0, \theta = 0 \quad at\ x = +f(\delta z)$$

3. ANALYSIS OF THE FLOW

Introduce the transformation such that

$$\bar{z} = \delta z, \frac{\partial}{\partial z} = \delta\frac{\partial}{\partial\bar{z}}$$

Then $\frac{\partial}{\partial z} \approx O(\delta) \to \frac{\partial}{\partial\bar{z}} \approx O(1)$

For small values of δ <<1, the flow develops slowly with axial gradient of order δ and hence we take $\frac{\partial}{\partial\bar{z}} \approx O(1)$.

Using the above transformation the equations (2.11) and (2.12) reduce to

$$F^4\psi - M_1^2 F^2\psi + \frac{G}{R}(\frac{\partial\theta}{\partial x}) = \delta R(\frac{\partial\psi}{\partial\bar{z}}\frac{\partial(F^2\psi)}{\partial x} - \frac{\partial\psi}{\partial x}\frac{\partial(F^2\psi)}{\partial\bar{z}}) \quad (3.1)$$

$$\delta PR(\frac{\partial\psi}{\partial x}\frac{\partial\theta}{\partial z} - \frac{\partial\psi}{\partial z}\frac{\partial\theta}{\partial x}) = ((1+\frac{4}{3N})\frac{\partial^2 T}{\partial x^2} + \delta^2\frac{\partial^2 T}{\partial z^2}) - \alpha\theta \quad (3.2)$$

Where $F^2 = \frac{\partial}{\partial x^2} + \delta^2\frac{\partial}{\partial\bar{z}^2}$

Assuming the slope δ of the wavy boundary to be small we take

$$\psi(x,z) = \psi_0(x,z) + \delta\psi_1(x,z) + \delta^2\psi_2(x,z) + \ldots\ldots\ldots\ldots \quad (3.3)$$

$$\theta(x,z) = \theta_o(x,z) + \delta\theta_1(x,z) + \delta^2\theta_2(x,z) + \ldots\ldots\ldots\ldots \quad (3.4)$$

Let $\eta = \frac{x}{f(\bar{z})}$

Substituting (3.3) in equations (3.1) and (3.2) and using (3.4) and equating the like powers of δ the equations and the respective boundary conditions to the zeroth order are

$$\frac{\partial^2\theta_0}{\partial\eta^2} - (\alpha_1 f^2)\theta_0 = 0 \quad (3.5)$$

$$\frac{\partial^4\psi_0}{\partial\eta^4} - (M_1^2 f^2)\frac{\partial^2\psi_0}{\partial\eta^2} = -\frac{Gf^3}{R}(\frac{\partial\theta_0}{\partial\eta}) \quad (3.6)$$

with

$$\psi_0(+1) - \psi_0(-1) = 1$$
$$\frac{\partial\psi_0}{\partial\eta} = 0,\ \frac{\partial\psi_0}{\partial\bar{z}} = 0,\quad \theta_0 = 1 \quad at \quad \eta = -1 \quad (3.7)$$
$$\frac{\partial\psi_0}{\partial\eta} = 0,\ \frac{\partial\psi_0}{\partial\bar{z}} = 0,\quad \theta_0 = 0 \quad at \quad \eta = +1$$

and to the first order are

$$\frac{\partial^2\theta_1}{\partial\eta^2} = PRf\left(\frac{\partial\psi_0}{\partial\eta}\frac{\partial\theta_0}{\partial\bar{z}} - \frac{\partial\psi_0}{\partial\bar{z}}\frac{\partial\theta_0}{\partial\eta}\right) \tag{3.8}$$

$$\frac{\partial^4\psi_1}{\partial\eta^4} - (M_1^2 f^2)\frac{\partial^2\psi_1}{\partial\eta^2} = -\frac{Gf^3}{R}\left(\frac{\partial\theta_1}{\partial\eta}\right) + Rf\left(\frac{\partial\psi_0}{\partial\eta}\frac{\partial^3\psi_0}{\partial z^3} - \frac{\partial\psi_0}{\partial\bar{z}}\frac{\partial^3\psi_0}{\partial x\partial z^2}\right) \tag{3.9}$$

with

$$\begin{aligned} &\psi_1(+1) - \psi_1(-1) = 0 \\ &\frac{\partial\psi_1}{\partial\eta} = 0,\ \frac{\partial\psi_1}{\partial\bar{z}} = 0, \quad \theta_1 = 0 \quad at \quad \eta = -1 \\ &\frac{\partial\psi_1}{\partial\eta} = 0,\ \frac{\partial\psi_1}{\partial\bar{z}} = 0, \quad \theta_1 = 0 \quad at \quad \eta = +1 \end{aligned} \tag{3.10}$$

4. SOLUTION OF THE PROBLEM

Solving the equations (3.5) and (3.6) subject to the boundary conditions (3.7).we obtain

$$\theta_0 = 0.5\left(\frac{Ch(h\eta)}{Ch(h)} - \frac{Sh(h\eta)}{Sh(h)}\right)$$

$$\psi_0 = a_7 Cosh(\beta_1\eta) + a_8 Sinh(\beta_1\eta) + a_9\eta + a_{10} + \phi_1(\eta)$$

$$\phi_1(\eta) = a_3\eta\, Sh(h\eta) + a_8 Ch(h\eta) + a_5\eta Ch(h\eta) + a_6 Sh(h\eta)$$

Similarly the solutions to the first order are

$$\begin{aligned} &\theta_1 = b_1 Ch(h\eta) + b_2 Sh(h\eta) + \phi_2(\eta) \\ &\phi_2(\eta) = a_{71} - a_{72}\eta - a_{73}\eta^2 - (a_{74} + \eta a_{75} + \eta^2 a_{76})Sh(h\eta) + (\eta a_{77})Ch(h\eta) + \\ &\quad + (a_{80} + a_{81}\eta + a_{82}\eta^2)Ch(2h\eta) + (-a_{78} + a_{79}\eta)Sh(2h\eta) + \\ &\quad + (a_{83} + a_{87}\eta)Sh(\beta_2\eta) + (a_{84} + a_{88}\eta)Sh(\beta_3\eta) + (a_{85} + a_{89}\eta)x \\ &\quad xCh(\beta_2\eta) + (a_{86} + a_{90}\eta)Ch(\beta_3\eta) \end{aligned}$$

$$\psi_1 = b_3 Cosh(\beta_1\eta) + b_4 Sinh(\beta_1\eta) + b_5\eta + b_6 + \phi_3(\eta)$$

$$\begin{aligned}\phi_3(\eta) = {} & a_{211}Sh(h\eta) + a_{212}Ch(h\eta) + a_{213}\eta Sh(h\eta) + a_{214}\eta Ch(h\eta) + a_{215}\eta^2 Ch(h\eta) \\ & + a_{216}Sh(2h\eta) + a_{217}Ch(2h\eta) + a_{218}\eta Sh(h\eta) + a_{211}Sh(h\eta) + a_{219}\eta Ch(2h\eta) \\ & + a_{220}\eta^2 Sh(2h\eta) + a_{221}Ch(\beta_2\eta) + a_{222}\eta Ch(\beta_2\eta) + a_{223}Sh(\beta_2\eta) + a_{224}\eta Sh(\beta_2\eta) \\ & + a_{225}\eta Ch(\beta_2\eta) + a_{226}Ch(\beta_3\eta) + a_{227}Sh(\beta_3\eta) + a_{228}\eta Sh(\beta_3\eta) + a_{229}\eta Sh(\beta_3\eta) \\ & + a_{230}yCh(\beta_1\eta) + a_{231}ySh(\beta_1\eta) + a_{232} + a_{233}\eta + a_{234}\eta^2 + a_{235}\eta^3 + a_{236}\eta^4 + a_{237}\eta^5\end{aligned}$$

where $a_1, a_2, \ldots\ldots\ldots\ldots, a_{237}, b_1, b_2, \ldots\ldots\ldots\ldots, b_6$ are constants given in the appendix.

5. SHEAR STRESS AND NUSSELT NUMBER

The shear stress on the channel walls is given by

$$\tau = \frac{(f^2(1+f'^2)\psi_{0,\eta\eta} + \delta(f^2(1+f'^2)\psi_{1,\eta\eta} - (2f'/f)\psi_{0,x\eta}) + O(\delta^2)}{(1+f'^2)}$$

and the corresponding expressions are

$$(\tau)_{\eta=+1} = \frac{(f^2(1+f'^2)b_3 + \delta(f^2(1+f'^2)b_5 - (2f'/f)b_1) + O(\delta^2)}{(1+f'^2)}$$

$$(\tau)_{\eta=-1} = \frac{(f^2(1+f'^2)b_4 + \delta(f^2(1+f'^2)b_6 - (2f'/f)b_2) + O(\delta^2)}{(1+f'^2)}$$

The rate of heat transfer (Nusselt Number) on the walls has been calculated using the formula

$$Nu = \frac{1}{f(\theta_m - \theta_w)}\left(\frac{\partial\theta}{\partial\eta}\right)_{\eta=\pm1}$$

where $\theta_m = 0.5\int_{-1}^{1}\theta\, d\eta$

$$(Nu)_{\eta=+1} = \frac{1}{f\theta_m}(a_{93} + \delta(a_{95}))$$

$$(Nu)_{\eta=-1} = \frac{1}{f(\theta_m - 1)}(a_{94} + \delta(a_{96}))), \quad \theta_m = a_{80} + \delta\, a_{81}$$

6. RESULTS AND DISCUSSION OF THE NUMERICAL RESULTS

We investigate the effect of Hall Currents and radiation on convective heat transfer flow of a viscous electrically conducting fluid in a vertical non uniform channel in the presence of heat source. The geometry of the channel wall is taken as $y=1+\beta \exp(-x^2)$, $\beta > 0$ corresponds dilation and $\beta < 0$ corresponds to constriction of the pipe. The walls are maintained at constant temperatures. The axial velocity 'w' is shown in fig 1-7 for different values of G, R,β, M, m, α, N and z.

The actual axial flow is in the vertically upward direction and hence $w < 0$ represents a reversal flow. Fig. 1 represents the variation of w with Grashoff number 'G'. A reversal flow is noticed with increase in $G < 0$ and region of the reversal flow enlarges with increase in |G|. Also |w| experiences an enhancement with increase in |G| and maximum 'w' is attained at $\eta = -0.2$. An increase in the Reynolds number 'R' depreciates |w| everywhere in the flow region (fig. 2). The variation of 'w' with Hartmann number 'M' and Hall parameter 'm' shows that higher the Lorentz force larger |w| in the flow region. An increase in $m \leq 2.5$ accelerates 'w' and further increase in $m \geq 3.5$ results in a depreciation in the axial velocity in flow region (fig.3). The variation of w with heat source parameter 'α' shows that an increase in the strength of heat generating source results in a depreciation in |w| (fig. 4). With reference to variation of 'w' with β we find that greater the constriction of channel wall higher |w| in the region (fig. 5). An increase in the radiation parameter N leads to a depreciation in w. The depreciation in w for smaller values of N is remarkable and marginal for higher values of 'N' (fig. 6). The variation of 'w' with axial distance 'z' shows that a reversal flow is observed with increase in $z \geq \pi/2$ and the region of the reversal flow decreases with $z \leq \pi$ and enhances with higher $z \geq 2\pi$. Also |w| depreciates with increase in $z \geq 2\pi$ (fig. 7).

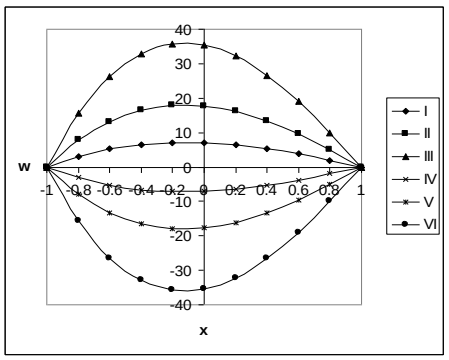

Fig. 1 : Variation of w with G

	I	II	III	IV	V	VI
G	10^3	$3x10^3$	$5x10^3$	-10^3	$-3x10^3$	$-5x10^3$

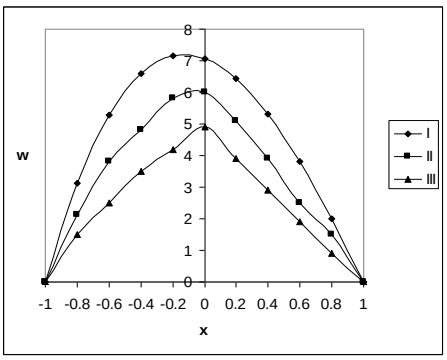

Fig. 2 : Variation of w with R

	I	II	III
R	10^2	$2x10^2$	$3x10^2$

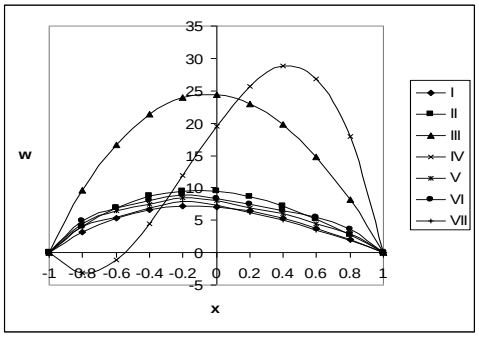

Fig. 3 : Variation of w with M, m

	I	II	III	IV	V	VI	VII
M	2	4	6	10	0.2	0.2	0.2
m	0.5	0.5	0.5	0.5	1.5	2.5	3.5

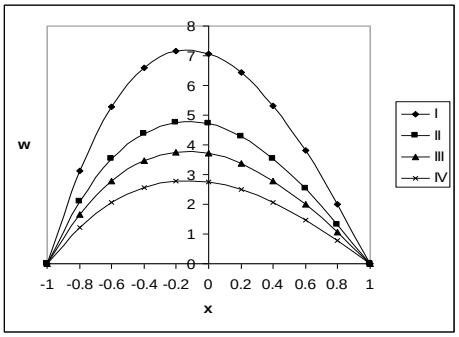

Fig. 4 : Variation of w with α

	I	II	III	IV
α	2	4	6	10

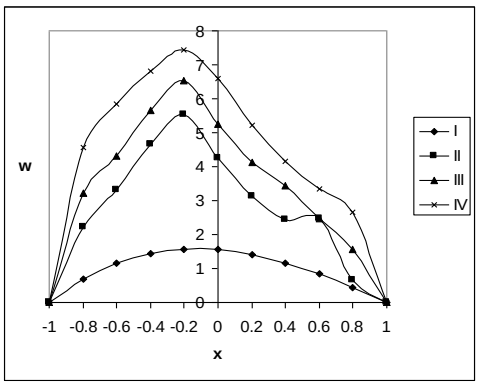

Fig. 5 : Variation of w with β

	I	II	III	IV
β	-0.3	-0.5	-0.7	-0.9

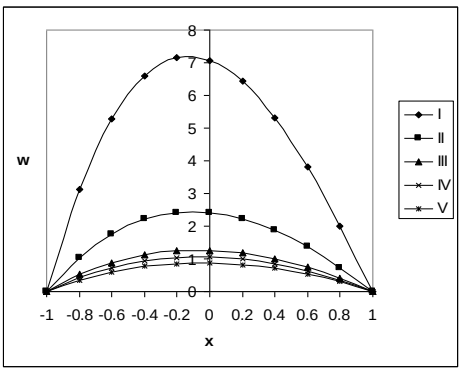

Fig. 6 : Variation of w with N

	I	II	III	IV	V
N	1.5	1.5	5	10	100

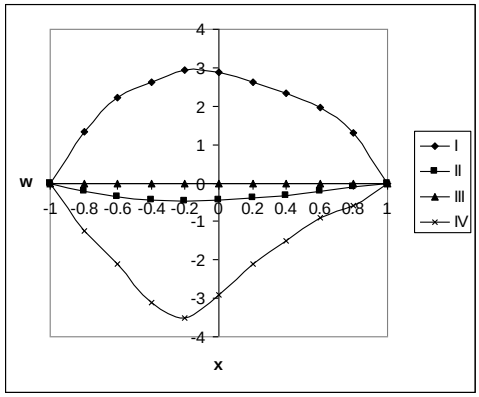

Fig. 8: Variation of u with G

	I	II	III	IV	V	Vi
G	10^3	$3x10^3$	$5x10^3$	-10^3	$-3x10^3$	$-5x10^3$

The secondary velocity 'u' which is due to waviness of the boundary is shown in fig 8-14 for different parametric values. Fig. 8 represents variation of 'u' with 'G'. It is found that for G > 0 the flow is towards the mid region and is towards the boundary for G > 0. The magnitude of 'u' enhance with increase |G| with maximum attained at $\eta = 0$. An increase in R enhances |u| in the flow region (fig. 9). Figure 10 shows the variation of 'u' with M and m. It is noticed that higher the strength of the magnetic field larger is 'u' in the flow region. An increase in the Hall parameter for $m \leq 2.5$ enhances 'u' and depreciates with higher $m \geq 3.5$ (fig.10). From fig. 11 we notice a decreasing tendency in 'u' with an increase in the strength of the heat source. The influence of the surface geometry on 'u' is shown in fig. 12. It is found that higher the constriction of the channel values larger |u| in the flow region. With reference to variation of 'u' with radiation heat flux we find that an increase in radiation parameter 'N' results in a depreciation in |u|. Thus the presence of the radiative heat transfer depreciates the secondary velocity in the flow region (fig. 13). The variation of 'u' with axial distance 'z' shows that for $z \leq \pi/2$ the secondary velocity is towards the boundary and for higher values of $z \geq \pi$ it is towards mid region. Also |u| depreciates with increase in $z \leq \pi$ and enhances with higher $z \geq 2\pi$ (fig 14).

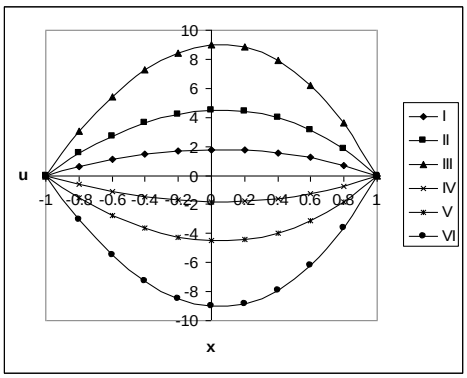

Fig. 8: Variation of u with G

	I	II	III	IV	V	Vi
G	10^3	$3x10^3$	$5x10^3$	-10^3	$-3x10^3$	$-5x10^3$

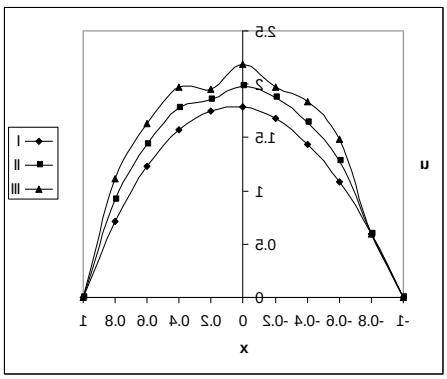

Fig. 9: Variation of u with R

	I	II	III
R	10^2	$2x10^2$	$3x10^2$

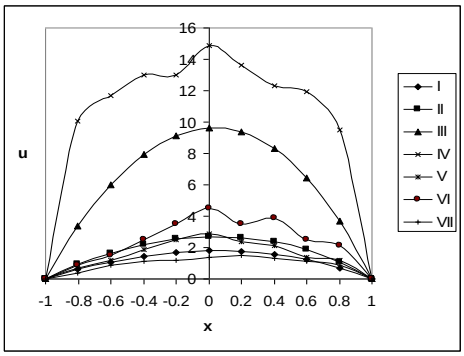

Fig. 10 : Variation of u with M, m

	I	II	III	IV	V	VI	VII
M	2	4	6	10	0.2	0.2	0.2
m	0.5	0.5	0.5	0.5	1.50	2.50	3.50

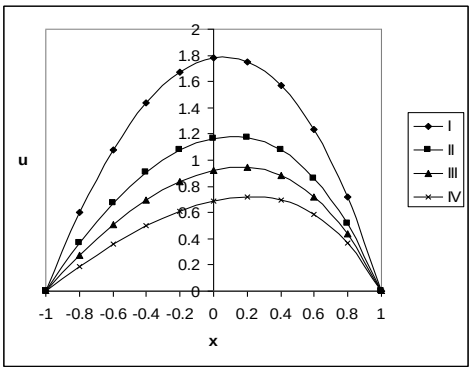

Fig. 11 : Variation of u with α

	I	II	III	IV
α	2	4	6	10

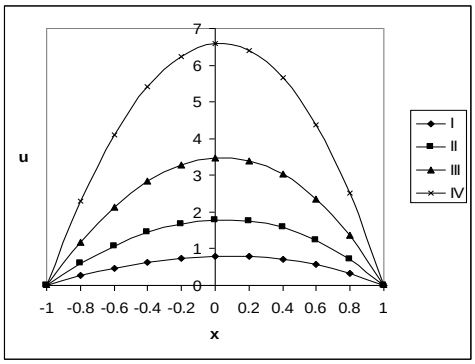

Fig. 12: Variation of u with β

	I	II	III	IV
β	-0.3	-0.5	-0.7	-0.9

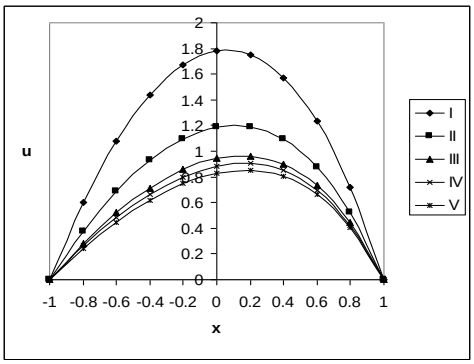

Fig. 13: Variation of u with N

	I	II	III	IV	V
N	0.5	1.5	5	10	100

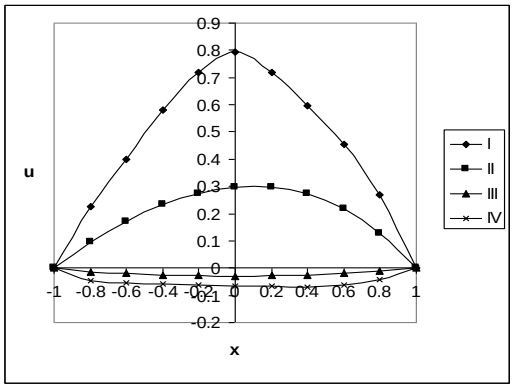

Fig. 14: Variation of u with z

	I	II	III	IV
Z	$\pi/4$	$\pi/2$	π	2π

The non-dimensional temperature distribution (θ) is shown in fig. 15-21 for different parameters. We follow the convention that the non-dimensional temperature is negative or positive according as the axial temperature is greater/lesser than T_2. Fig. 15 represents the variation of 'θ 'with Grashoff number G. It is found that axial temperature enhances with increase in G. An increase in the Reynolds number 'R' enhances the axial temperature (fig.16). From fig.17 it is found that higher the strength of the magnetic field ($M \leq 6$) smaller the axial temperature and for further increase in the intensity of strength ($M \geq 10$) larger the actual temperature. An increase in Hall parameter $m \leq 2.5$ results in a depreciation in the axial temperature and for further enhancement in $m \geq 3.5$ we notice an enhancement in the axial temperature everywhere in the flow region (fig.17). The variation of 'θ' with heat source parameter 'α' shows that the axial temperature enhances with $\alpha \leq 6$ and depreciates with higher $\alpha \geq 10$ (fig.18). The influence of the surface geometry on 'θ' is shown in fig. 19. It is observed that higher the constriction of the channel walls larger the axial temperature in flow region. An increase in the radiation parameter N leads to a depreciation in the axial temperature (fig.20). Thus we notice that the inclusion of the radiative heat transfer reduces the axial temperature in the flow region. Moving along the axial direction of channel the actual temperature depreciates with $z \leq \pi/2$ and enhances with $z \geq \pi$ (fig.21).

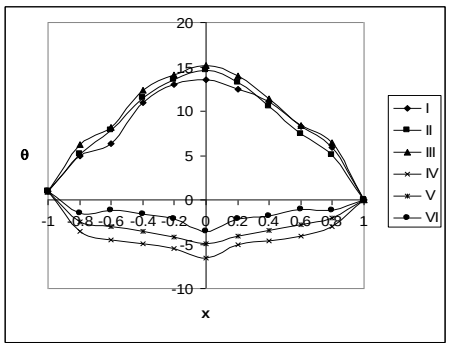

Fig. 15 : Variation of θ with G

	I	II	III	IV	V	VI
G	10^3	$3x10^3$	$5x10^3$	-10^3	$-3x10^3$	$-5x10^3$

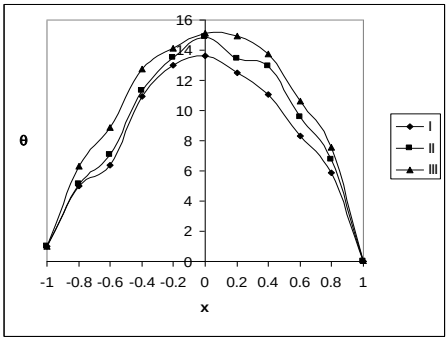

Fig. 16 : Variation of θ with R

	I	II	III
R	10^2	$2x10^2$	$3x10^2$

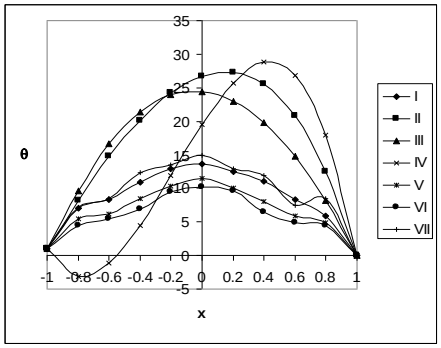

Fig. 17: Variation of θ with M, m

	I	II	III	IV	V	VI	VII
M	2	4	6	10	0.2	0.2	0.2
m	0.5	0.5	0.5	0.5	1.5	2.5	3.5

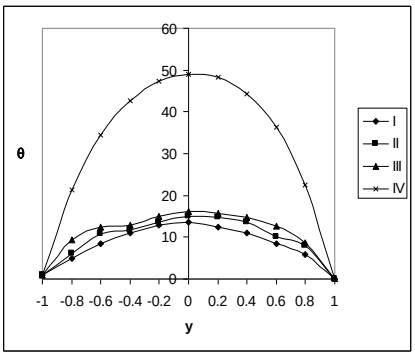

Fig. 18: Variation of θ with α

	I	II	III	IV
α	2	4	6	10

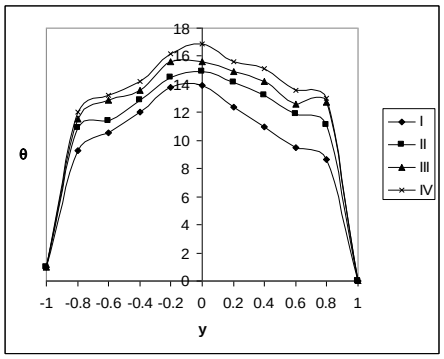

Fig. 19: Variation of θ with β

	I	II	III	IV
β	-0.3	-0.5	-0.7	-0.9

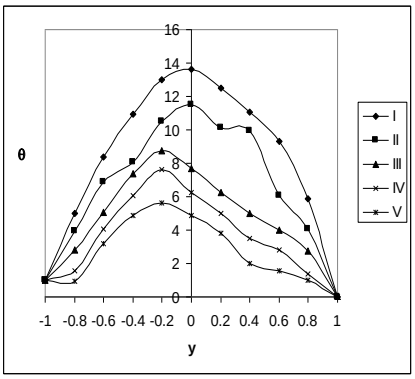

Fig. 20: Variation of θ with N

	I	II	III	IV	V
N	1.5	1.5	5	10	100

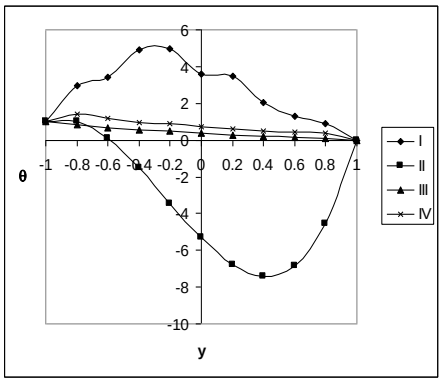

Fig. 21 : Variation of θ with z

	I	II	III	IV
z	π/4	π/2	π	2π

The stress (τ) at η = ±1 is evaluated for different values of G, M, m, α, β, N, R, z and are shown in tables 1-6. The variation of τ with Grashoff number 'G' shows that an increase in G > 0 reduces |τ| at η = ±1 while it enhances at η = +1 and depreciates at η = -1 with increase in |G|. The variation of τ with M shows that higher the strength of magnetic field larger the |τ| at both the walls. An increase in the Hall parameter m ≤ 1.5 reduces |τ| and enhances with higher m ≥ 2.5 at η = +1 and at η = -1 |τ| enhances with 'm' for all 'G'. Variation of τ with 'α' reveals that |τ| enhances at η = +1 and reduces at η = -1 with increase in the strength of heat source (tables 1 and 4). The influence of surface geometry on the stress is shown in tables 2 and 5. Higher the constriction of the channel walls smaller is |τ| and for further lowering of the constriction larger |τ| at η = +1 and at η = -1 larger |τ| for all G. An increase in the radiation parameter N results an enhancement of |τ| at η = +1 while at η = = -1, |τ| enhances with N ≤ 1.5 and depreciates for higher N ≥ 5. From tables 3 and 6 we find that the stress reduces at η = +1 and enhances at η = -1 for G > 0 and for G < 0 it reduces with R at both the walls. Moving along the axial direction of the channel walls the stress enhances with z ≤ π/2 and depreciates with higher z ≥ π and η = -1 it reduces with z. In general, we notice that the stress at η = -1 is much larger than that at η = 1.

The average Nusselt number (Nu) which measures the rate of heat transfer across the boundaries is shown in tables 7-12 for different variations. It is observed that the rate of heat

transfer enhances with increase in |G| at $\eta = \pm 1$. An increase in M enhances |Nu| at $\eta = +1$ and at $\eta = -1$, |Nu| reduces with $M \leq 4$ and enhances with $M \geq 6$. Also the rate of heat transfer depreciates with increase in Hall parameter 'm'. With reference of Nu with heat source parameter 'α', we find a decay in the magnitude of Nu with increase in 'α', at both the walls (tables 7 and 10). The influence of surface geometry on Nu is exhibited in tables 8 and 10. Higher the constriction of the channel walls larger is the rate of heat transfer at both the walls. An increase in the radiation parameter $N \leq 1.5$ reduces |Nu| and enhances with higher $N \geq 5$ and at $\eta = -1$ the rate of heat transfer decays in magnitudes (tables 8 and 11). The variation of Nu with Reynolds number 'R' shows that |Nu| reduces with R at $\eta = +1$ while at $\eta = -1$, |Nu| enhances with $R \leq 70$ and reduces with $R \geq 140$. Moving along the axial direction the Nusselt number at $\eta = +1$ reduces with $z \leq \pi/2$ and enhances with $z \geq \pi$, while at $\eta = -1$ it reduces with 'z' for all G (tables 9 and 12).

In general, we find that the rate of heat transfer at $\eta = -1$ is much larger than that $\eta = +1$.

Table-1
Shear stress (τ) at $\eta = +1$

G	I	II	III	IV	V	VI	VII
10^3	0.588	1.177	12.723	0.259	0.689	0.594	0.602
$5x10^3$	0.175	3.046	32.031	0.075	0.275	1.464	1.532
-10^3	-0.096	-1.316	-13.020	-0.066	-0.961	-0.612	-0.639
$-5x10^3$	-0.212	-3.186	-32.328	-0.202	-0.262	-1.504	-1.569
M	2	4	6	2	2	2	2
M	0.5	0.5	0.5	1.5	2.5	0.5	0.5
α	2	2	2	2	2	4	6

Table-2
Shear stress (τ) at $\eta = +1$

G	I	II	III	IV	V	VI
10^3	0.110	0.059	0.635	0.470	0.509	0.525
$5x10^3$	0.321	0.175	1.605	1.203	1.299	1.492
-10^3	-0.170	-0.096	-0.659	-0.507	-0.546	-0.563
$-5x10^3$	-0.380	-0.212	-1.630	-1.241	-1.337	-1.429
β	-0.3	-0.5	-0.7	-0.5	-0.5	-0.5
N	0.5	0.5	0.5	1.5	5	10

Table-3
Shear stress (τ) at η= +1

G	I	II	III	IV	V	VI
10^3	0.059	0.329	-0.259	-0.169	0.039	0.029
$5x10^3$	0.175	-0.201	-0.19	-0.19	0.145	0.125
-10^3	-0.096	-0.428	-0.259	-0.159	-0.066	-0.048
$-5x10^3$	-0.212	-0.259	-0.169	-0.149	-0.112	-0.102
Z	π/4	π/2	π	2π	π/4	π/4
R	100	100	100	100	200	300

Table-4
Shear stress (τ) at η= -1

	I	II	III	IV	V	VI	VII
10^3	-16.63	-28.49	-38.49	-16.9	-17.21	-15.39	-14.36
$5x10^3$	-15.50	-253.96	-39.33	-15.5	-15.50	-13.49	-12.30
-10^3	-17.39	-26.22	-40.84	-17.39	-18.39	-15.08	-13.10
$-5x10^3$	-15.96	-25.75	-39.06	-14.96	-15.96	-14.08	-125.98
M	2	4	6	2	2	2	2
M	0.5	0.5	0.5	1.5	2.5	0.5	0.5
α	2	2	2	2	2	4	6

Table-5
Shear stress (τ) at η= -1

G	I	II	III	IV	V	VI
10^3	-17.46	-16.63	-19.21	-19.38	-15.17	-15.56
$5x10^3$	-14.137	-15.50	-18.39	-14.69	-12.91	-12.02
-10^3	-15.57	-17.39	-19.76	-16.88	-15.06	-14.82
$-5x10^3$	-14.37	-16.96	-18.53	-14.69	-12.82	-12.00
β	-0.3	-0.5	-0.7	-0.5	-0.5	-0.5
N	0.5	0.5	0.5	1.5	5	10

Table-6
Shear stress (τ) at η= +-1

G	I	II	III	IV	V	VI
10^3	-16.63	83.57	14.85	0.323	-16.38	-16.51
$5x10^3$	-16.50	-12.278	9.152	-0.165	-15.59	-15.63
-10^3	-17.39	-12.94	-3.678	-0.205	-17.13	-16.04
$-5x10^3$	-16.96	-11.17	-7.928	-0.15	-16.85	-15.82
z	π/4	π/2	π	2π	π/4	π/4
R	100	100	100	100	200	300

Table-7
Nusselt number (Nu) at η= +1

G	I	II	III	IV	V	VI	VII
10^3	0.779	2.690	4.717	0.679	0.579	-0.175	-0.295
$5x10^3$	1.975	6.831	8.015	1.675	1.475	-0.410	-0.711
-10^3	-0.816	-2.829	-3.014	-0.616	-0.516	0.138	0.258
$-5x10^3$	-2.013	-6.969	-4.312	-1.812	-1.613	0.373	0.674
M	2	4	6	2	2	2	2
M	0.5	0.5	0.5	1.5	2.5	0.5	0.5
α	2	2	2	2	2	4	6

Table-8
Nusselt number (Nu) at η= +1

G	I	II	III	IV	V	VI
10^3	0.201	0.779	1.60	-0.157	-0.298	-0.311
$5x10^3$	0.546	1.975	4.02	-0.364	-0.716	-0.749
-10^3	-0.260	-0.816	-1.63	0.119	0.260	0.274
$-5x10^3$	-0.606	-2.012	-4.05	0.327	0.679	0.712
β	-0.3	-0.5	-0.7	-0.5	-0.5	-0.5
N	0.5	0.5	0.5	1.5	5	10

Table-9
Nusselt number (Nu) at η= +1

G	I	II	III	IV	V	VI
10^3	0.779	-0.016	-0.159	-0.179	0.679	0.778
$5x10^3$	1.975	-0.064	-0.259	-0.299	1.675	1.475
-10^3	-0.816	-0.084	-0.169	-0.179	-0.616	-0.516
$-5x10^3$	-2.01	-0.059	-0.289	-0.299	-1.812	-1.612
Z	π/4	π/2	π	2π	π/4	π/4
R	100	100	100	100	200	300

Table-10
Nusselt number (Nu) at η= -1

G	I	II	III	IV	V	VI	VII
10^3	15.58	10.06	5.73	4.29	3.97	14.68	13.71
$5x10^3$	16.71	14.88	6.56	5.71	4.71	15.89	14.30
-10^3	14.88	13.60	5.34	4.88	3.88	13.83	12.38
$-5x10^3$	15.26	14.58	6.31	5.26	4.26	14.52	13.98
M	2	4	6	2	2	2	2
m	0.5	0.5	0.5	1.5	2.5	0.5	0.5
α	2	2	2	2	2	4	6

Table-11
Nusselt number (Nu) at η= -1

G	I	II	III	IV	V	VI
10^3	9.16	15.58	18.54	8.20	9.27	9.19
$5x10^3$	13.87	15.71	18.33	13.49	12.11	12.36
-10^3	11.68	14.88	17.92	11.83	9.89	9.63
$-5x10^3$	12.13	15.26	18.17	13.02	12.59	11.82
β	-0.3	-0.5	-0.7	-0.5	-0.5	-0.5
N	0.5	0.5	0.5	1.5	5	10

Table-12
Nusselt number (Nu) at η= -1

G	I	II	III	IV	V	VI
10^3	15.58	9.81	8.4	-0.534	14.84	13.69
$5x10^3$	15.71	11.84	0.386	0.622	15.92	14.58
-10^3	14.88	10.82	-4.669	0.422	14.99	13.18
$-5x10^3$	15.26	4.69	-1.51	0.522	16.36	15.39
z	π/4	π/2	π	2π	π/4	π/4
R	100	100	100	100	200	300

7. REFERENCES

[1]. Chandrasekhar, S.: Hydrodynamic and Hydromagnetic stability, Claranden press, Oxford (1961)

[2]. Comini. G, C. Nomino and S. Savino.: Convective heat and mass transfer in wavy finned-tube exchangers, Int. J. Num. Methods for heat and fluid flow. V.12 (6), pp.735-755(2002)

[3]. David Moleam.: Steady state heat transfer with porous medium with temperature dependent heat generation, Int. J. Heat and Mass transfer,V.19, pp.529(1976)

[4]. Deshikachar, K. S. and Ramachandra Rao, A.: Effect of a magnetic field on the flow and blood oxygenation in channel of variables cross section, Int.J. Engg.Sci, V.23, pp.1121 (1985)

[5]. Hyon Gook Wan, Sang Dong Hwang, Hyung He Cho.: Flow and heat /mass transfer in a wavy duct with various corrugation angles in two-dimensional flow. Heat and Mass transfer, V.45, pp. 157-165(2008)

[6]. Jer - huan Jang and Wei - mon Yan.: Mixed convection heat and mass transfer along a vertical wavy surface, Int. j. heat and mass transfer, v.47,i.3, pp.419-428(2004)

[7].Mahdy, A.: Mixed convection heat and mass transfer on a vertical wavy plate embedded in a saturated porous medium (PST/PSE), Int.J. Appl. Maths and Mech, V. 5, (7), pp. 88-97(2008)

[8]. McMichael, M and Deutch, S.: Phys. Fluids, V.27, pp.110 (1984)

[9].Palm, E. Weber, J.E and Kvernold, O.: On steady convection in a porous medium, F F M, V.30, pp.33-40(1972)

[10]. Rao, D. R. V, Krishna, D. V and Debnath, L.: Combined effect of free and forced convection on MHD flow in a rotating porous channel, Int. J. Maths and Math. Sci, V.5, pp.165-182(1982)

[11]. Sree Ramachandra Murthy, A.: Buoyancy induced hydromagnetic flows through a porous medium-A study, Ph.D thesis, S. K. University, Anantapur, A.P, India (1992)

[12]. Vajravelu, K and Sastry, K. S.: Forced convective heat transfer in a viscous incompressible fluid confined between a long vertical wavy wall and parallel flat wall, J. fluid. Mech, v. 86(20), pp.365 (1978)

[13]. Vajravelu, K. and Debnath, L.: Non-linear study of convective heat transfer and fluid flows induced by traveling thermal waves, Acta Mech, V.59, pp. 233-249(1986).

[14]. Vajravelu, K and Neyfeh, A. H.: Influence of wall waviness on friction and pressure drop in channels, Int. J. Mech and Math.Sci.V.4, N0.4, pp.805-818 (1981).